Chapter 3

Lysine Dendrimers and Their Complexes with Therapeutic and Amyloid Peptides: Computer Simulation

Elena Popova, Dilorom Khamidova, Igor Neelov and Faizali Komilov

Additional information is available at the end of the chapter

http://dx.doi.org/10.5772/intechopen.71052

Abstract

Lysine dendrimers consist of natural lysine amino acid residues. Due to this reason, they are usually not as toxic as other dendrimers. Lysine dendrimers are often used in drug and gene delivery. These dendrimers penetrate blood-brain barrier and thus could be used for the delivery of drugs and other substances, for example, bioactive peptides to brain or elimination of disease-related peptides out of the brain. To do it, dendrimers should form complex with these peptides. In the present chapter, we describe computer simulation of the interaction of lysine dendrimer of the second generation with three different peptides and check does it form complexes with them. Two of these peptides (Semax and Epithalon) are nootropic peptides and third is the fragment of amyloid peptide, which forms amyloid fibrils and plaques in Alzheimer's disease. Our simulation demonstrates that the lysine dendrimers form complexes with these therapeutics peptides. Thus, we demonstrated that lysine dendrimer is a good candidate for the delivery of therapeutic peptides. We also have shown that lysine dendrimer destroys existing stacks of amyloid peptides and forms a stable complex with them. Thus, it looks that it could be used in future for the treatment of Alzheimer's diseases.

Keywords: lysine dendrimer, peptide delivery system, molecular dynamics, Semax, Epithalon

1. Introduction

Only a few of the peptide drugs reach their targets. Most of them accumulate in nontargeted organs and produce different side-effects. Drug delivery systems help to overcome these

problems and increase safety and efficacy of therapeutic peptides [1]. Traditional drug delivery systems include tablets, injections, suspensions, ointments, creams, liquids, and aerosols. Polymers are also used for this goal and protect drugs from biological degradation during delivery [2].

Dendrimers were synthesized in seventieth to eightieth of the last century [3]. They have regular branched (star-like) structure. Dendrimers have well-defined size and constant spherical shape. Many dendrimers have a large number of charged terminal groups available for functionalization [4, 5]. Dendrimers could be used for drug and gene delivery, as a branched core for multiple antigen peptides (MAPs) as well as antibacterial and antiviral agents. Also, they were proposed as potent anti-amyloid agents for the treatment of different neurodegenerative diseases (Alzheimer's, Parkinson's, etc.).

In the present chapter, we describe our results of simulation of the interaction of the second generation lysine dendrimer (**Figure 1**) with three types of peptides: Semax, Epithalon, and the fragment of amyloid peptide.

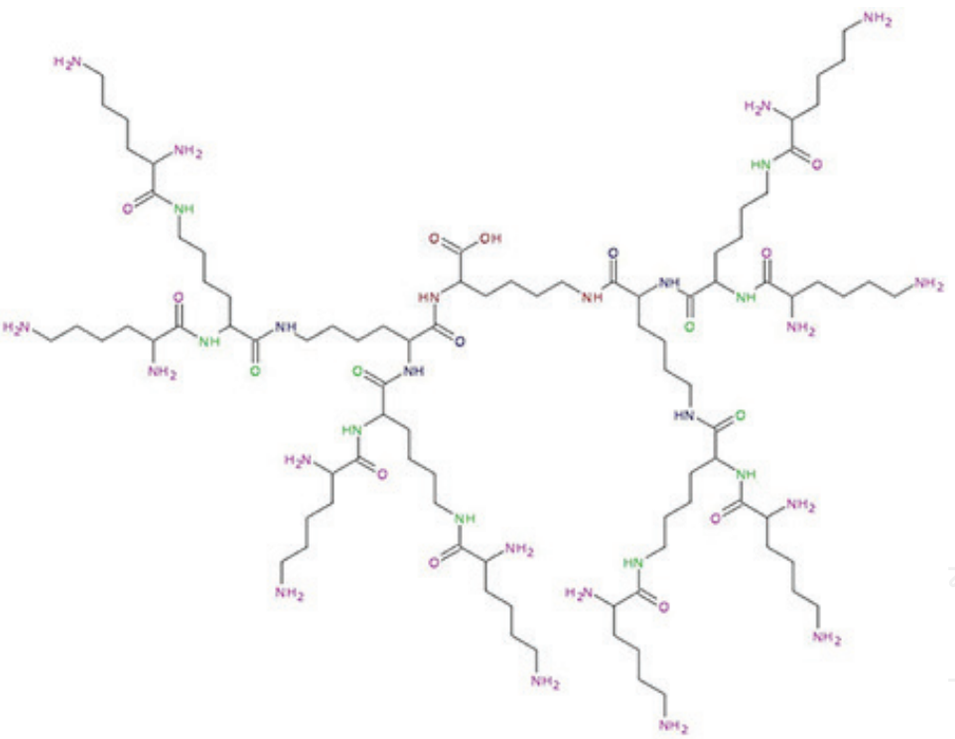

Figure 1. Structure of lysine dendrimer of the second generation.

2. Molecular dynamics simulation

Molecular dynamics simulation (MDS) is widely used for modeling of different polymer and biopolymer systems. In this approach, all atoms or groups of atoms in molecules in a system are represented by spherical beads. Chemical bonds between atoms are represented by

springs or rigid bonds. The dynamics of such mechanical model of real molecular systems is described by classical Newton equations of motion and the system of these equations for all beads in the system is solved numerically.

$$F_i = m_i \frac{d^2 r_i(t)}{dt^2} \quad (1)$$

where $r_i(t) = (x_i(t), y_i(t), z_i(t))$—the position vector of the ith particle (or its coordinates $x_i(t)$, $y_i(t)$, $z_i(t)$), F_i—the force acting on the ith particle at time t, and m_i—mass of the particle.

This method was applied for the first time for the study of simple 2D model of hard disks, which represents two-dimensional analog of a monoatomic gases [6]. Later, it was extended for simulation of liquids [7, 8] and coarse-grained model of linear polymer chains [9] and n-alkanes [10]. During the last 30 years, MDS was applied for the study of many molecular systems of different structure and composition. The potential energy in MDS usually includes the energy of valence bonds, the energy of valence angles, and dihedral angles as well as van der Waals energy and electrostatic energies. In the present study, the variant of molecular dynamics simulation approach realized in the framework of GROMACS 4.5.6 software package [11] and one of the most modern force fields (AMBER_99SB-ildn) was used for the representation of potential energy [12] of our system. The force field has the following form:

$$U(r_1, \ldots, r_N) = \sum \frac{a_i}{2}(l_i - l_{i0})^2 + \sum \frac{b_i}{2}(\theta_i - \theta_{i0})^2 + \sum \frac{c_i}{2}[1 + \cos(n\omega_i - \gamma_i)] + \sum 4\varepsilon_{ij}\left[\left(\frac{\sigma_{ij}}{r_{il}}\right)^{12} - \left(\frac{\sigma_{ij}}{r_{il}}\right)^{6}\right] + \sum k \frac{q_i q_j}{r_{ij}} \quad (2)$$

where l_i—valence bond lengths, θ_i—valence angles values, l_{i0} and θ_{i0}—equilibrium values of them, and a_i and b_i—force constants, correspondingly, $\varepsilon_{ij}$and σ_{ij}—values of Van der Waals parameters of Lenard-Jones 6–12 potential, q_i—partial charges, c_i, γ_i, and n—numerical coefficients in dihedral potential while summation is done through all i-beads or pairs of ith and jth beads in the system consisting of N beads.

The more detailed description of MDS method used in the present work including simulation of linear and branched polyelectrolytes as well as dendrimers has been described in [13–33]. All simulations were performed at normal conditions (temperature 300 K and pressure 1 atm).

The size of dendrimer and complexes at time t was evaluated by the mean square radius of gyration $R_g(t)$ which is defined from:

$$R_g^2(t) = \frac{1}{M} \times \left[\sum_{i=1}^{N} m_i \times |r_i(t) - R|^2\right], \quad (3)$$

where R—the center of mass of subsystem, r_i and m_i—coordinates and masses of i-atom correspondingly, N—the total number of atoms in subsystem, and M—the total mass of dendrimer. This function was calculated using *g_gyrate* function of GROMACS software.

Radial distribution of density $p(r)$ of atoms in dendrimer and complexes as well as distribution of ion pairs were calculated using g_rdf function of the GROMACS package.

To calculate the coefficient of translational mobility of dendrimer and complexes, the time dependence of the mean square displacements of the centers of inertia (MSD) of corresponding subsystem was calculated. MSD was calculated using g_msd function of GROMACS.

$$\left\langle \sum_t \Delta r^2(t + k\Delta t) \right\rangle = \left\langle (r(t + k\Delta t) - r(t))^2 \right\rangle = 6Dt \quad (4)$$

3. Semax peptide

Therapeutic Semax peptide with primary sequence Met-Glu-His-Phe-Pro-Gly-Pro [34] was selected in present chapter as the first peptide for study. Semax is one of the few synthetic regulatory peptides that, after all the fundamental research, have found its application in therapy as a nootropic and neuroprotective agent [35]. However, its penetration into the brain and mechanisms of action remain insufficiently studied. In addition, the peptide is rapidly destroyed by blood enzymes [36].

To check if lysine dendrimer forms a complex with Semax peptides, we prepared system containing lysine dendrimer of the second generation, 16 Semax peptides, and counterions in water and studied the time evolution of this system.

Snapshots of this system are shown in **Figure 2** at different time moments during MD simulation (water molecules are not shown for clarity). It is easy to see that at the beginning of the time trajectory (**Figure 2a**), all peptide molecules are located far from the dendrimer. After 20 ns (**Figure 2b**), some peptide molecules already sit on the surface of the dendrimer, and at the end of the simulation (**Figure 2c**), most of the peptide molecules are adsorbed on its surface.

The time dependence of gyration radius $R_g(t)$ (**Figure 3a**) shows that at the beginning of simulation, the size of subsystem consisting of lysine dendrimer and Semax peptides is big because peptides are located far from dendrimer. During first 30–40 ns, the value of $R_g(t)$ decreases

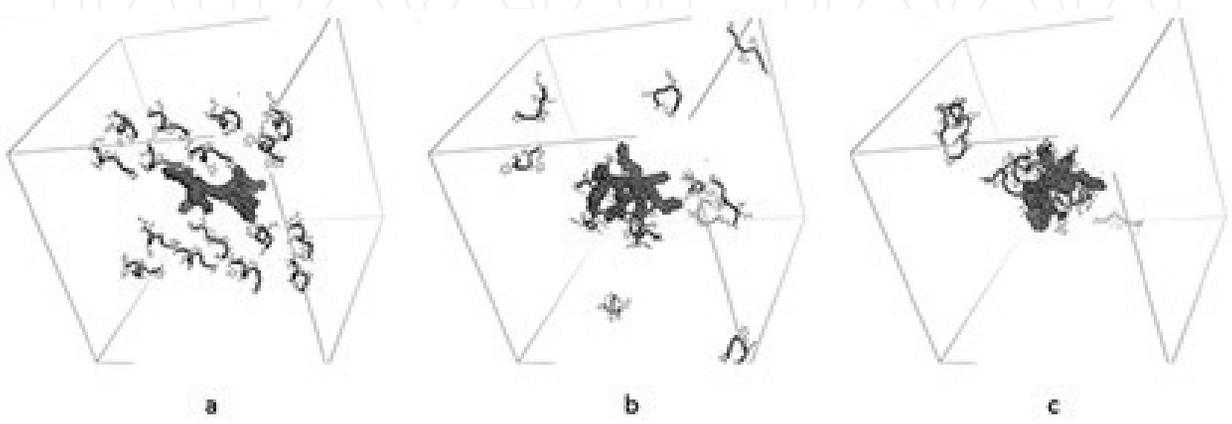

Figure 2. Snapshots of the dendrimer and Semax peptides at different time moments: $t = 0$ (a), $t = 20$ ns (b), $t = 160$ ns (c).

because peptides begin to adsorb on dendrimer surface. Stable dendrimer-peptides complex forms within 30–40 ns and after this time the size of complex fluctuates but its average value does not change with time.

Another quantity that can characterize complex formation is the hydrogen bond number (N) between dendrimer and peptides (see **Figure 3b**). In the beginning of simulation, there are no contacts between dendrimer and peptides and hydrogen bond number between them equals zero. The increase of this function with time during first 30–40 ns demonstrates that the number of contacts between dendrimer and peptides increases due to complex formation and after this time it fluctuates but its average value almost does not change with time. Thus, from **Figure 3b**, we can conclude that the system reaches equilibrium (plateau) state after 30–40 ns. This result correlates well with results for the gyration radius in **Figure 3a**.

We also calculated different equilibrium characteristics (see **Table 1** and **Figure 4**) of complex averaged through equilibrium part of our simulation ($t > 40$ ns). In particular, we calculated the mean square radius of gyration R_g of our dendrimer and complex (consisting of G2 and 16 Semax peptides) and obtained that the value of R_g of the complex is nearly twice larger than the size of dendrimer itself (see **Table 1**). It is quite natural because the molecular weight of the complexes also increases nearly twice in comparison with the molecular weight of the dendrimer. The shape of dendrimer and complex can be characterized by main components of the tensor of inertia R_g^{11}, R_g^{22}, R_g^{33}, (see **Table 1**). It can be roughly estimated by ratio R_g^{33}/R_g^{11} of largest and smallest eigenvalues of inertia tensor of the corresponding subsystem. The ratio is equal to 1.68 for dendrimer and 1.45 for dendrimer with peptides. Thus, we obtained that complex has more spherical shape than dendrimer.

The radial density distribution functions are shown in **Figure 4a**. It demonstrates that atoms of dendrimer (curve 2, **Figure 4a**) are located mainly in the center (i.e. at small distances r from the center of mass), whereas peptides (curve 1, **Figure 4**) are mainly on the surface of the

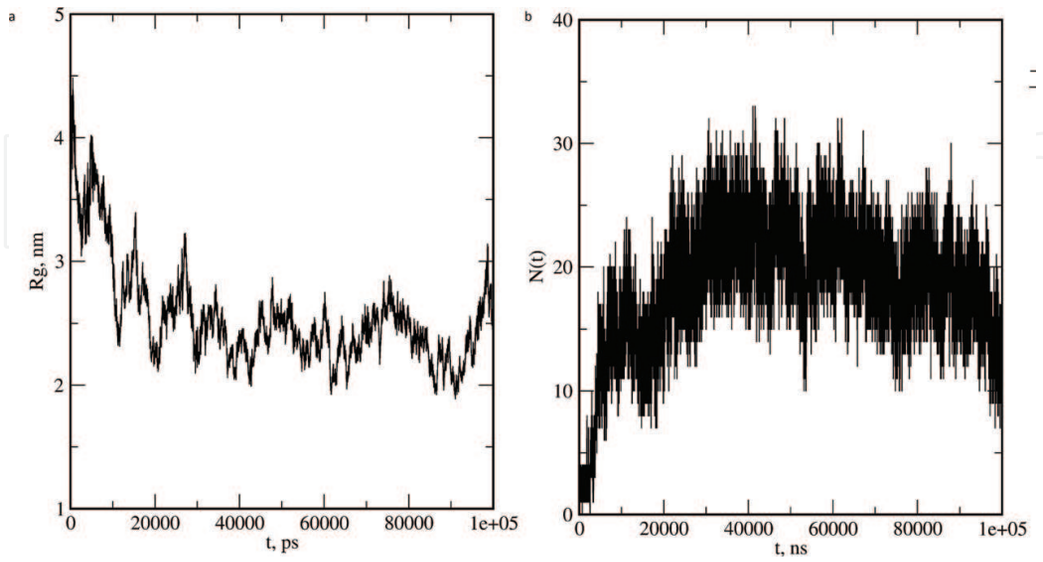

Figure 3. Time dependence of gyration radius of subsystem consisting of dendrimer and peptides (a) and time dependence of number of hydrogen bonds (N) between dendrimer and peptides during the complex formation (b).

System	R_g^{11} (nm)	R_g^{22} (nm)	R_g^{33} (nm)	R_g (nm)
Dendrimer (G2)	0.64	0.97	1.08	1.12
G2 + 16 Semax	1.36	1.88	1.97	2.30

Table 1. Eigenvalues R_g^{11}, R_g^{22}, R_g^{33} of tensor of inertia in dendrimer and Semax peptide complex.

complex. At the same time, some fraction of peptides could slightly penetrate into dendrimer but not to its inner part.

The average number of hydrogen bonds between peptides and dendrimers in the equilibrium state (which was determined from second part (t > 40 ns) of **Figure 3b**) shows how tightly peptides are connected with dendrimer. From our calculations, it follows that average hydrogen bonds number in equilibrium state for the complex is close to 19. It means that each peptide is connected in average by one hydrogen bond with dendrimer. We could also check how the number of hydrogen bonds in the equilibrium state fluctuates. It is easy to see from **Figure 3b** that fluctuations in hydrogen bond number between dendrimer and peptides in the complex are in the range of 8–30. It means that the average number of hydrogen bonds with dendrimer per peptide fluctuates between 0 and 2.

Another equilibrium characteristic of interaction between dendrimer and peptides in the complex is the distribution of ion pair numbers between their oppositely charged groups. **Figure 4b** shows the dependence of ion pair number on the distance between dendrimer charges and peptides charges (curve 1) in the complex as well as between dendrimer charges and counterions (curve 2). It is seen, that there is a sharp peak, corresponding to the direct contact

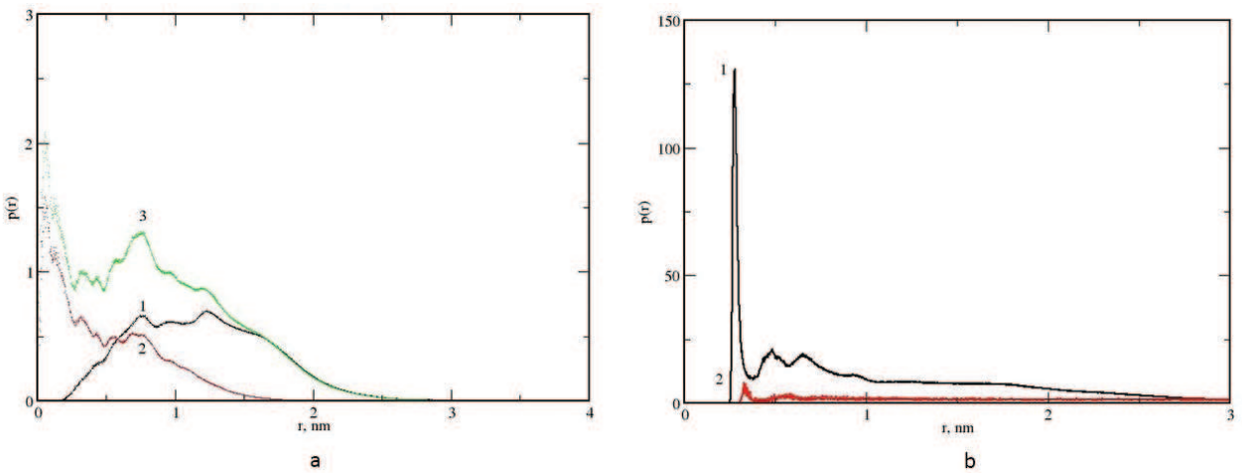

Figure 4. Radial distribution functions $p(r)$: density distribution of the atoms in the complex: 1—peptide atoms, 2—dendrimer atoms, 3—all atoms of the complex (a) and distribution function of ion pair numbers between opposite charges: 1—between NH_3^+ groups of the dendrimer and COO^- groups of peptides; 2—between NH_3^+ groups of the dendrimer and Cl− ions (b).

between positively charged groups (NH_3^+) of dendrimer and negatively charged groups (COO^-) of the glutamic acid in peptides (curve 1) and peak between dendrimer charges and counterions is less pronounced (curve 2). It means that dendrimer and peptides are strongly connected by this ion pairs with each other, whereas dendrimer charges and counterions contacts are not so strong.

To determine diffusion coefficient of the dendrimer-peptide complex, we calculated its mean square displacement (MSD) as a function of time. It was obtained, that the time dependence of MSD function is close to linear in double logarithm coordinates (not shown). It means that the translational motion of complex is the diffusion-like motion. The diffusion coefficient of the complex was determined from the slope of the time dependence of MSD and it is equal to $(0.12 \pm 0.03) \times 10^5$ sm^2/s.

The results of simulation of the system consisting of lysine dendrimer of the second generation and 16 Semax peptides confirm that lysine dendrimer quickly forms complex with these peptides and thus lysine dendrimers could be a good candidate for using as a vehicle for delivery of Semax peptides.

4. Epithalon peptides

Therapeutic peptide Epithalon was selected in present chapter as the second model peptide. Biologically active regulatory peptides are promising and effective medicines in a wide range of diseases treatment. Such peptides are effective at low concentrations, selective, multifunctional, and completely biodegradable and do not produce side-effects [37]. Epithalon is a regulatory tetrapeptide with amino acid sequence of alanine-glutamate-asparagine-glycine (AENG). It is synthesized as analogs of the epithalamine peptide preparation and isolated from the epiphysis of the animal brain [38].

One of the most important properties of this peptide is its ability to activate the telomerase enzyme in patients' body and to prolong human cells life. The most well-known pharmacological properties of Epithalon are the following:

1. Regulation of neuroendocrine system.
2. Increased sensitivity of hypothalamus to endogenous hormonal effects.
3. Normalization of gonadotropin hormones, uric acid, and cholesterol level.
4. Strengthening of the immune system.
5. Inhibition of spontaneous and induced carcinogenesis.
6. Improves rheological properties of blood and reduces formation of blood clots.

To check if lysine dendrimer could form the complex with Epithalon peptides, we prepared system consisting of lysine dendrimer of second generation, 16 Epithalon peptides, counterions, and water and studied time evolution of this system.

Snapshots of a system consisting of dendrimers, peptides, and ions during simulation are shown in **Figure 5** (water molecules are not shown for clarity). It is easy to see that at the beginning of process (**Figure 5a**) peptide molecules located far from dendrimer. After 20 ns (**Figure 5b**), some part of the peptide molecules are already sitting on the surface of the dendrimer, and in the end (**Figure 5c**) most of the peptide molecules adsorbed on its surface. This behavior is very similar to that for the system consisting of dendrimer and Semax peptides discussed above.

The time dependence of radius of gyration $R_g(t)$ describes the process of transition of the system to equilibrium state with the formation of a complex between dendrimer and Epithalon peptides (see **Figure 6a**). From **Figure 6a**, one can see that at the beginning of simulation the size of subsystem consisting of dendrimer and peptides is big because peptides are far from dendrimer. During first 20–30 ns, the value of $R_g(t)$ decreases because peptides begin to adsorb on dendrimer surface and after this time the average value of R_g practically does not change with time. It means that stable dendrimer-peptides complex forms within 20–30 ns.

Another quantity that can characterize complex formation is the hydrogen bond number $N(t)$ between dendrimer and peptides (see **Figure 6b**). In the beginning of simulation, there are no contacts between dendrimer and peptides and the number of hydrogen bonds between them equals zero. The increase of this function with time during first 20–30 ns demonstrates that the number of contacts between dendrimer and peptides increases due to complex formation. From **Figure 6b**, we can conclude that the complex goes into an equilibrium (plateau) state after 30–40 ns. This result correlates well with the results for the gyration radius $R_g(t)$ in **Figure 6a**.

After equilibration and complex formation, all characteristics of complex fluctuate but their average values practically do not change with time. We calculated different equilibrium characteristics of complex averaged through these equilibrium part of our simulation ($t > 30$ ns).

It was obtained that in equilibrium state the size R_g of the complex (G2 and 16 Epithalon peptides) is near 2.18 times larger than the size of dendrimer itself. The shape of the complex can

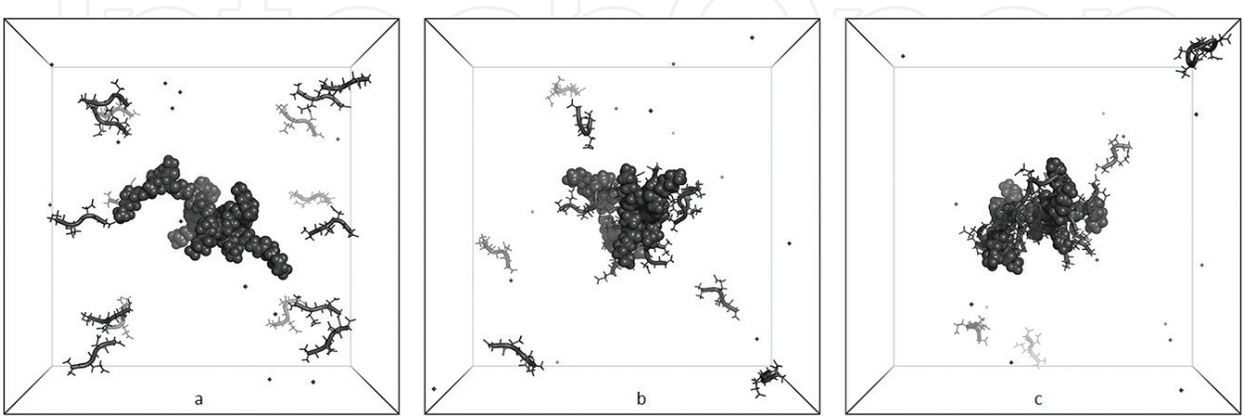

Figure 5. Time evolution of dendrimer and Epithalon peptides during complex formation: $t = 0$ (a), $t = 20$ ns (b), $t = 160$ ns (c).

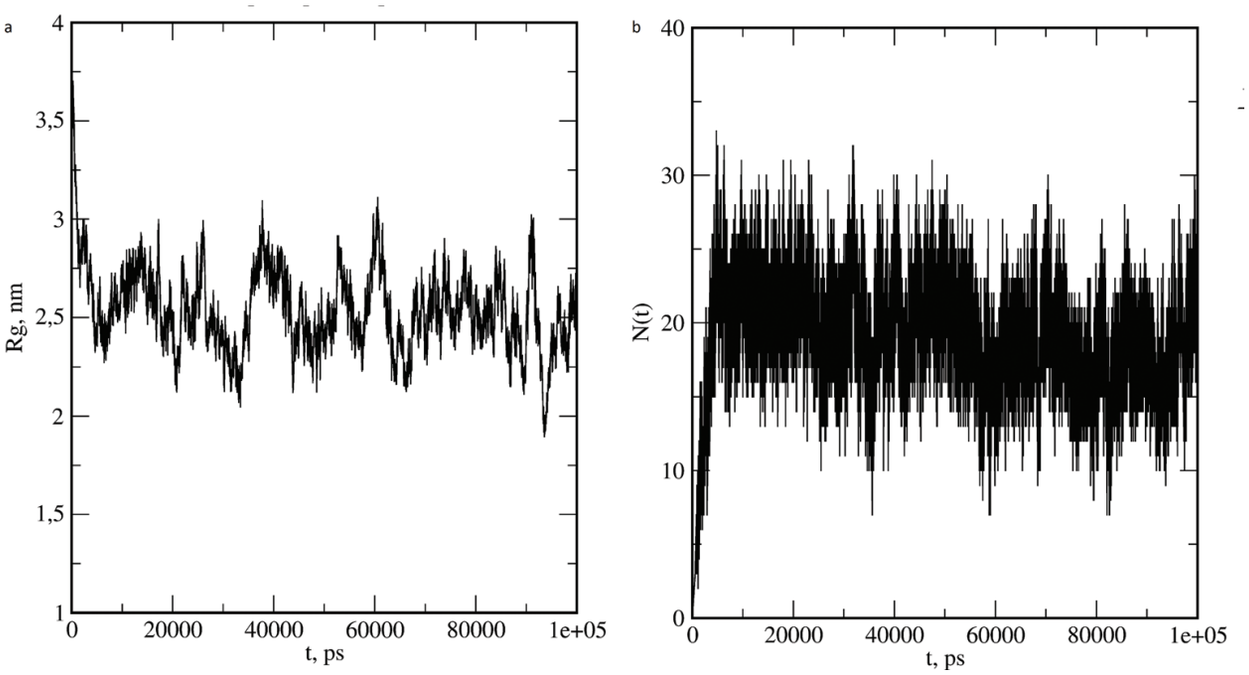

Figure 6. Time dependence of gyration radius $R_g(t)$ of subsystem consisting of the dendrimer and Epithalon peptides (a) and time dependence of number of hydrogen bonds (N) between dendrimer and Epithalon peptides during the complex formation (b).

System	R_g^{11} (nm)	R_g^{22} (nm)	R_g^{33} (nm)	R_g (nm)
Dendrimer (*G*2)	0,64	0,97	1,08	1,12
*G*2 + 16 Epithalon	1.76	2.08	2.26	2.44

Table 2. Eigenvalues R_g^{11}, R_g^{22}, R_g^{33} of tensor of inertia in dendrimer and Epithalon peptide complex.

be characterized by main components of the tensor of inertia R_g^{11}, R_g^{22}, R_g^{33} (see **Table 2**). In the simplest case, anisotropy can be characterized by R_g^{33}/R_g^{11}. For dendrimer, this ratio is equal to 1.69 and for the complex—1.28. Thus, the anisotropy of dendrimer with adsorbed Epithalon peptides is less than anisotropy of dendrimer itself as it was shown earlier for the complex of dendrimer with Semax peptides.

The equilibrium ($t > 30$ ns) radial density distribution functions $p(r)$ are shown in **Figure 7a**. It demonstrates that atoms of dendrimer (curve 2, **Figure 7a**) located in the center of the complex (i.e. at small distances r from the center of mass) and Epithalon peptides (curve 1, **Figure 7a**) located mainly on the surface of the complex. At the same time, some fraction of peptides could slightly penetrate into dendrimer but not to its inner part.

The average number of hydrogen bonds between dendrimer and Epithalon peptides in the equilibrium state (which was determined by averaging through $t > 30$ ns of **Figure 6b**) shows how tightly peptides are associated with dendrimer. From our calculations, it follows

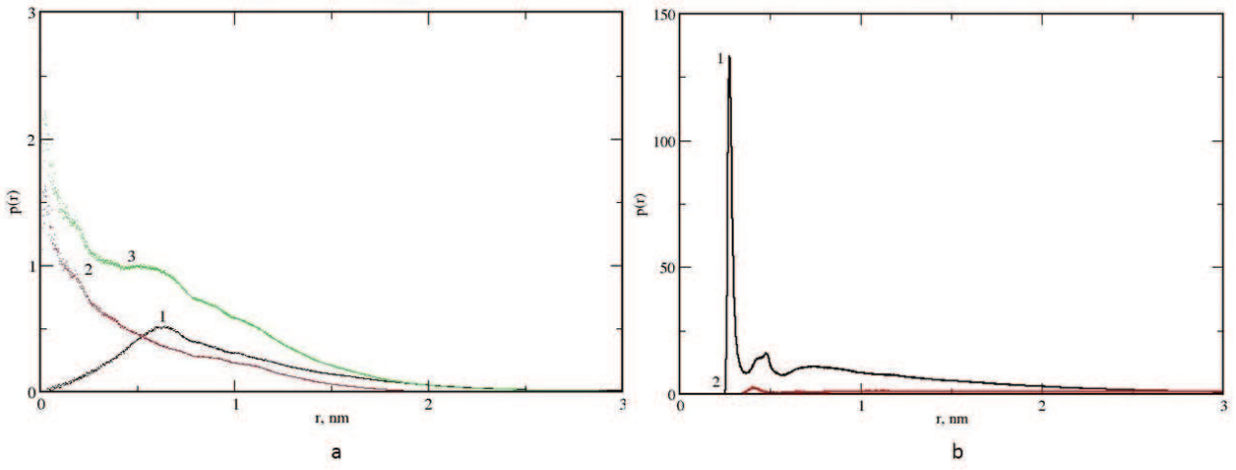

Figure 7. Radial distribution functions $p(r)$: density distribution of atoms in complex: 1—peptide atoms; 2—dendrimer atoms; 3—all atoms of the complex (a) and distribution function of ion pair numbers between opposite charges: 1—between NH_3^+ groups of the dendrimer and COO^- groups of peptides; 2—between NH_3^+ groups of the dendrimer and counterions (b).

that average hydrogen bond number in equilibrium state for the complex is close to 20. It means that each peptide is connected in average by one hydrogen bond with dendrimer. We also could check how the number of hydrogen bonds in the equilibrium state fluctuates. Fluctuations in hydrogen bonds number between dendrimer and peptides in the complex (see **Figure 6b**) are in the range of 9–28. It means that the average number of hydrogen bonds with dendrimer per peptide fluctuate between 0 and 2.

Figure 7b shows the dependence of ion pair numbers on the distance between dendrimer charges and Epithalon peptides charges in the complex as well as between dendrimer charges and counterions. It is seen that there is a sharp peak, corresponding to the direct contact between positively charged groups (NH_3^+) of dendrimer and negatively charged groups (COO^-) of peptides (curve 1) and significantly less sharp peak (curve 2) between dendrimer charges and counterions. It means that dendrimer and peptides are strongly connected at these points with each other, whereas dendrimer charges and counterions contacts are not so strong.

To determine diffusion coefficient of the dendrimer-peptide complex, we calculated its mean square displacement (MSD) as a function of time. It was obtained, that the time dependence of MSD function is close to linear in double logarithm coordinates (not shown). It means that the translational motion of complex is the diffusion-like motion. The diffusion coefficient of the complex was determined from the slope of the time dependence of MSD and is equal to $(0.21 \pm 0.03) \times 10^5$ sm^2/s.

The results of simulation of the system consisting of lysine dendrimer and Epithalon peptides confirm that the dendrimer could form complex with these peptides and thus lysine dendrimers could be a good candidate for using as a vehicle for delivery of Epithalon peptides.

5. Amyloid fibrils

Fragment of amyloid peptide (LVFFAE) was selected in present chapter as a third model peptide. Many peptides and proteins have the ability to self-assembly into amyloid fibrils. Polypeptides that can form amyloid fibrils include molecules associated with neurodegenerative diseases [39, 40]. For example, in Alzheimer's disease, it is a β-amyloid peptide, in Parkinson's disease, it is a-synuclein protein, and in type 2 diabetes mellitus, it is an islet-amyloid peptide (IAPP, or amylin). The most studied are amyloid peptides that are also called amyloid-β peptides or Aβ-peptides.

It is known that synthetic protonated dendrimers (for example, polyamidoamine (PAMAM) dendrimers) can prevent aggregation of amyloid peptides [41]. It was also shown that they can destroy already existing amyloid fibrils in solution. Recently, it was experimentally shown that lysine dendrimers can also destroy amyloid fibrils [14].

To confirm the possibility of amyloid stack destruction by lysine dendrimer, we prepared system consisting of lysine dendrimer of second generation and 16 short amyloid peptides (LVFFAE) in water with counterions and studied the time evolution of this system.

From snapshots in **Figure 8**, one can see that at the beginning of the process (**Figure 8a**) all peptide molecules of the stack are located rather far from the dendrimer. After 20 ns (**Figure 8b**), a few of peptide molecules are already detached from the stack and adsorbed on the surface of dendrimer, and in the end of calculations after 160 ns (**Figure 8c**), most of the peptide molecules in the system adsorbed on its surface.

The first part (t < 20–30 ns) of the time dependence of gyration radius $R_g(t)$ describes the process of destruction of the amyloid stack by G2 dendrimer and dendrimer-peptides complex formation (**Figure 9a**). From **Figure 9a**, one can see that second generation dendrimer forms complex with 16 peptides within 20–30 ns. After that, the complex size $R_g(t)$ fluctuates slightly, but its average value R_g practically does not change systematically with time. Therefore, we can assume that after 20–30 ns the system is in equilibrium state. It correlates with snapshots that are shown in **Figure 8**. From **Figure 9b**, it can be concluded that the system reaches equilibrium (plateau) state after 20–30 ns.

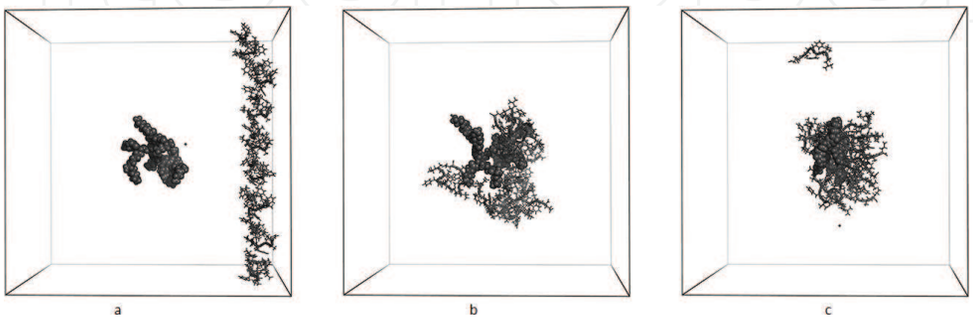

Figure 8. Snapshots of the LVFFAE stack and dendrimer at different time: t = 0 (a), t = 20 ns (b), t = 160 ns (c).

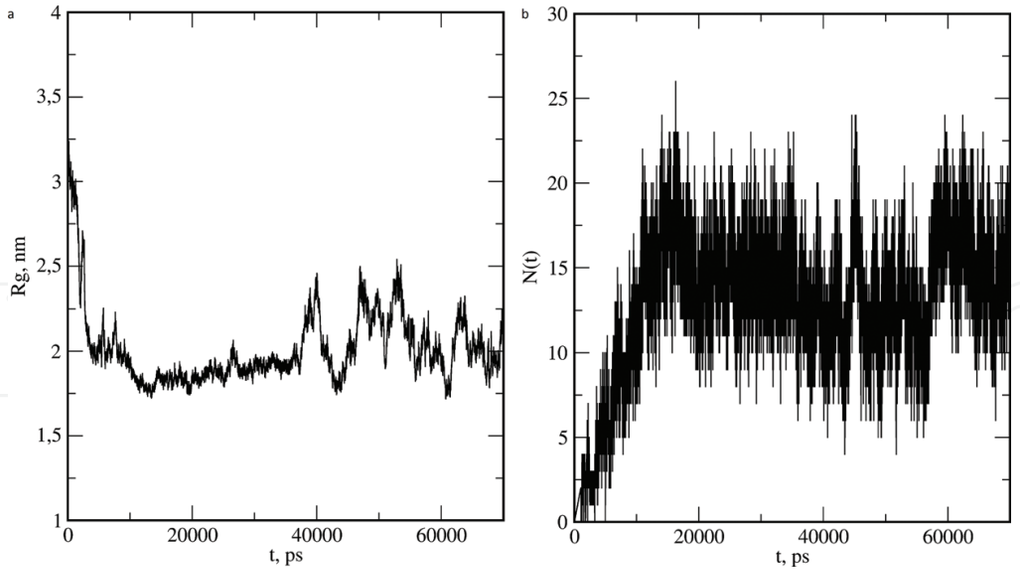

Figure 9. Time dependence of gyration radius of subsystem consisting of the dendrimer and peptides (a) and time dependence of hydrogen bonds number (*N*) between dendrimer and peptides during the complex formation (b).

The distance between neighboring peptides in amyloid stack (**Figure 10a**, curve 1) is an important characteristic of stability of the stack. The distance between dendrimer and peptides (**Figure 10a**, curve 2) allows estimating the rate of dendrimer-peptides complex formation after stack was destructed by dendrimer. At the beginning of simulation, the distances between the neighboring peptides of the stack are small. During first 20–30 ns, this distance is increase. It means that the destruction of amyloid stack occurs and peptides become separated from each other.

At the same time, the distance between dendrimer and peptides (**Figure 10a**, curve 2) in the beginning of the simulation (at $t = 0$) is large because peptides are located far from the

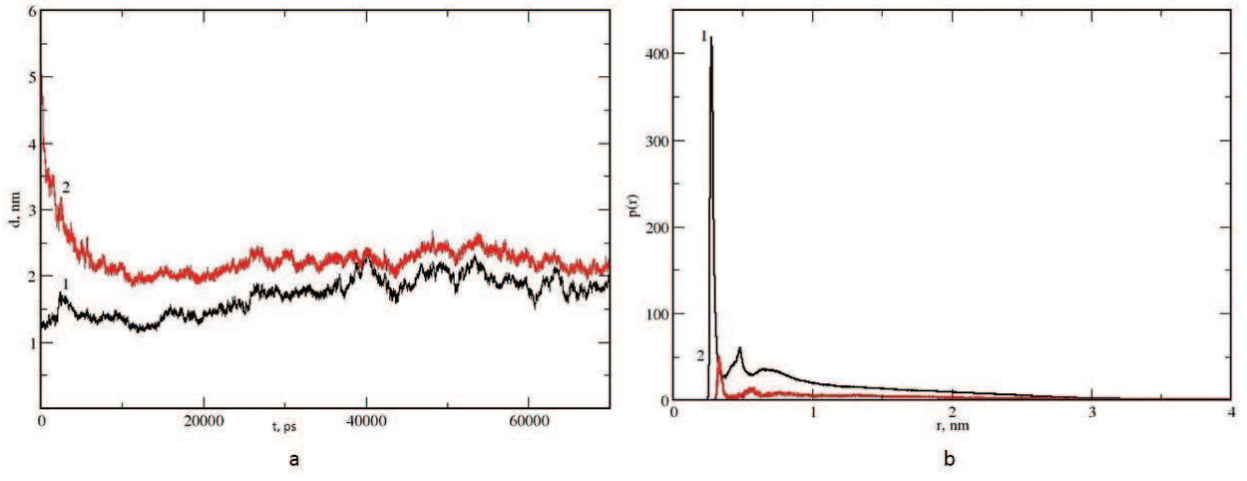

Figure 10. Changes in distances d between amyloid peptides (1) and between dendrimer and peptides (2) (a) and distribution function of ion pair numbers: 1—between NH_3^+ groups of the dendrimer and COO^- groups of peptides; 2—between NH_3^+ groups of the dendrimer and counterions (b).

dendrimer. During first 20–30 ns, the peptides become attracted by dendrimer and distance between them and dendrimer decreases. It means that the dendrimer of the second generation could destroy the stack of amyloid peptides and adsorb the peptides.

After complex formation (t > 20–30 ns), all characteristics of complex fluctuate but their average values do not change with time. We calculated different equilibrium characteristics of complex averaged through equilibrium part of our simulation (t > 30 ns).

In equilibrium state, the mean square radius of gyration R_g of the complex is 1.7 times larger than the size of the dendrimer G2 itself (see **Table 3**). The ratio R_g^{33}/R_g^{11} (which allows to roughly estimating anisotropy of molecule) is equal to 1.68 for dendrimer and 1.45 for the complex of dendrimer with peptides. Thus, the anisotropy of dendrimer with adsorbed amyloid peptides is again less than anisotropy of dendrimer itself as it was for previous two complexes of lysine dendrimer with model peptides Semax and Epithalon.

Radial distribution $p(r)$ density (not shown) obtained for this complex is similar to that for complexes of the dendrimer with two peptides (Semax and Epithalon) studied above. It demonstrates that dendrimer atoms are located mainly in the center of the complex and amyloid peptides are mainly on the surface of the complex. At the same time, some fraction of amyloid peptides could slightly penetrate into the outer part of the dendrimer.

The average number of hydrogen bonds N between dendrimer and LVFFAE peptides in our complex (determined from second part (t > 30 ns) of $N(t)$ from **Figure 9b**) is close to 15. It means that in average each amyloid peptide is connected by one hydrogen bond with dendrimer in the complex. Fluctuations in hydrogen bond number are in the range of 5–27, and it means that a number of hydrogen bonds per peptide can fluctuate between 0 and 2.

Figure 10b shows the dependence of number of ion pairs between dendrimer and peptide charges on the distance between them in the complex. One can see that there is a sharp peak, corresponding to the direct contact between positively charged groups (NH_3^+) of dendrimer and negatively charged groups (COO^-) in peptides (curve 1) and significantly less sharp peak between dendrimer charges and counterions (curve 2). It means that dendrimer and LVFFAE peptides are strongly connected at these points with each other, whereas dendrimer charges and counterions contacts are not so strong.

To determine diffusion coefficient of dendrimer-peptide complex, we calculated its mean square displacement (MSD) as a function of time. It was obtained that the time dependence of MSD function is close to linear in double logarithm coordinates (not shown). It means that the translational motion of complex is the diffusion-like motion. The coefficient of translational

System	R_g^{11} (nm)	R_g^{22} (nm)	R_g^{33} (nm)	R_g (nm)
Dendrimer (*G*2)	0,64	0,97	1,08	1,12
*G*2 + 16 LVFFAE	1,26	1,78	1,83	1,98

Table 3. Eigenvalues R_g^{11}, R_g^{22}, R_g^{33} of tensor of inertia in dendrimer and LVFFAE fibril complex.

diffusion of the complex was determined from the slope of the time dependence of MSD and is equal to $(0.13 \pm 0.04) \times 10^5$ sm^2/s.

The results of simulation of the system consisting of lysine dendrimer of second generation and fragments of amyloid peptides confirm that this lysine dendrimer could form the complex with amyloid peptides. Thus, lysine dendrimers could be a good candidate for using as anti-amyloid agent.

6. Conclusion

In the present chapter, we have shown that lysine dendrimer of the second generation could form stable complexes with therapeutic Semax and Epithalon peptides. We also have shown that this dendrimer could destroy the stable stacks of amyloid peptides and form stable complex with them. Thus, our simulations confirm that lysine dendrimers could be a good candidate for vehicles for the delivery of different nootropic peptides to brain and for the destruction of fibril consisting of disease-related peptides and elimination of them from the brain.

Acknowledgements

Computing resources for this study on supercomputers "Lomonosov" were provided by Supercomputer Centre of Moscow State University [42]. This work was supported by the grant of the Government of Russian Federation 074-U01 and by RFBR grant 16–03-00775.

Author details

Elena Popova[1,2], Dilorom Khamidova[3], Igor Neelov[2,4]* and Faizali Komilov[3]

*Address all correspondence to: i.neelov@mail.ru

1 Institute of Hygiene, Occupational Pathology and Human Ecology, St. Petersburg, Russia

2 ITMO University, St. Petersburg, Russia

3 Tajik National University, Dushanbe, Tajikistan

4 Institute of Macromolecular Compounds, St. Petersburg, Russia

References

[1] Caminade A-M, Turrin C-O, Laurent R, Ouali A, Delavaus-Nicot B. Dendrimers: Towards Catalitic, Material and Biomedical Uses. West Sussex, UK: A John Wiley & Sons, Ltd.; 2011. 515 p

[2] Bajpai AK, Bajpai J, Saini RK, Agrawal P, Tiwari A. Smart Biomaterial Devices. Polymers in Biomedical Sciences. Boca Raton: Taylor & Francis Group, LLC; 2017. 219 p

[3] Buhleier E, Wehner W, Vögtle F. "Cascade"- and "nonskid-chain-like" synthesis of molecular cavity topologies. Synthesis. 1978;**9**:155-158

[4] Kumar S, Pandita D. Dendrimers in drug delivery and targeting: Drug-dendrimer interactions and toxicity issues. Journal of Pharmacy and Bioalled Sciences. 2014;**6**(3):139-150

[5] Boas U, Sontjens SHM, Jensen KJ. New dendrimer-peptide host-guest complexes: Towards dendrimers as peptide carriers. Chembiochem. 2002;**3**(5):433-439

[6] Alder BJ, Wainwright TE. Molecular dynamics by electronic computers. In: Prigogine I, editor. International Symposium on Transport Processes in Statistical Mechanics. New York: Wiley Interscience; 1957. p. 97-131

[7] Verlet L. Computer "experiments" on classical fluids. I. Thermodynamical properties of Lennard-Jones molecules. Physics Review. 1967;**159**:98-103

[8] Rahman A, Stillinger FH. Molecular dynamics study of temperature effects on water structure and kinetics. The Journal of Chemical Physics. 1972;**57**:1281-1292

[9] Balabaev NK, Grivtsov AG, Shnol EE. Numerical Modeling of Motion of Molecules. Motion of Isolated Polymer Chain, preprint, Institute of Applied Mathematics. Moscow. 1972;**4**:38

[10] Ryckaert JP, Ciccotti G, Berendsen HJC. Numerical integration of Cartesian equations of motion of systems with constants-molecular dynamics of n-alkanes. Journal of Computational Physics. 1977;**23**:327-341

[11] Hess B, Kutzner C, Spoel D, Lindahl E. Gromacs 4: Algorithms for highly efficient, load-balanced, and scalable molecular simulation. Journal of Chemical Theory and Computation. 2008;**4**:435-447

[12] Hornak V, Abel R, Okur A, Strockbine D, Roitberg A, Simmerling C. Comparison of multiple amber force fields and development of improved protein backbone parameters. Proteins: Structure, Functions and Genetics. 2006;**65**:712-725

[13] Neelov I, Falkovich S, Markelov D, Paci E, Darinskii A, Tenhu H. Molecular Dynamics of Lysine Dendrimers. Computer Simulation and NMR. In: Dendrimers in Biomedical Applications. London: Royal Society of Chemistry; 2013. p. 99-114

[14] Neelov IM, Janaszewska A, Klajnert B, Bryszewska M, Makova N, Hicks D, Pearson H, Vlasov GP, Ilyash MY, Vasilev DS, Dubrovskaya NM, Tumanova NL, Zhuravin IA, Turner AJ, Nalieva NN. Molecular properties of lysine dendrimers and their interactions with Ab-peptides and neuronal cells. Current Medical Chemistry. 2013;**20**:134-143

[15] Markelov DA, Falkovich SG, Neelov IM, Ilyash MY, Matveev VV, Lahderanta E, Ingman P, Darinskii AA. Molecular dynamics simulation of spin-lattice NMR relaxation in poly-L-lysine dendrimers. Manifestation of the semiflexibility effect. Physical Chemistry and Chemical Physics. 2015;**17**:3214-3226

[16] Ennari J, Elomaa M, Neelov I, Sundholm F. Modelling of water free and water containing solid polyelectrolites. Polymer. 2000;**41**:985-990

[17] Ennari J, Neelov I, Sundholm F. Comparison of cell multipole and ewald summation methods for solid polyelectrolyte. Polymer. 2000;**41**:2149-2155

[18] Ennari J, Neelov I, Sundholm F. Molecular dynamics simulation of the peo sulfonic acid anion in water. Computational and Theoretical Polymer Science. 2000;**10**:403-410

[19] Ennari J, Neelov I, Sundholm F. Molecular dynamics simulation of the structure of PEO based solid polymer electrolytes. Polymer. 2000;**41**:4057-4063

[20] Ennari J, Neelov I, Sundholm F. Estimation of the ion conductivity of a PEO-based polyelectrolyte system by molecular modeling. Polymer. 2001;**42**(19):8043-8050

[21] Neelov I, Sundholm F. Modelling of gas transport properties of polymer electrolytes containing various amounts of water. Polymer. 2004;**45**:4171-4179

[22] Darinskii A, Gotlib Y, Lukyanov M, Neelov I. Computer simulation of the molecular motion in LC and oriented polymers. Progress in Colloid and Polymer Science. 1993;**91**:13-15

[23] Darinskii AA, Gotlib YY, Lyulin AV, Neelov IM. Computer modeling of polymer chain local dynamics in a field of a liquid crystal type. Vysokomolec. Soed. Ser. A. 1991;**33**:1211-1220

[24] Darinskii A, Lyulin A, Neelov I. Computer simulations of molecular motion in liquid crystals by the method of Brownian dynamics. Macromolecular Theory & Simulations. 1993;**2**:523-530

[25] Neelov IM, Adolf DB, Lyulin AV, Davies GR. Brownian dynamics simulation of linear polymers under elongational flow: Bead–rod model with hydrodynamic interactions. The Journal of Chemical Physics. 2002;**117**:4030-4041

[26] Neelov IM, Adolf DB. Brownian dynamics simulation of hyperbranched polymers under elongational flow. The Journal of Physical Chemistry. B. 2004;**108**:7627-7636

[27] Neelov IM, Adolf DB. Brownian dynamics simulations of dendrimers under elongational flow: Bead-rod model with hydrodynamic interactions. Macromolecules. 2003;**36**:6914-6924

[28] Sheridan PF, Adolf DB, Lyulin AV, Neelov I, Davies GR. Computer simulations of hyperbranched polymers: The influence of the Wiener index on the intrinsic viscosity and radius of gyration. The Journal of Chemical Physics. 2002;**117**:7802-7812

[29] Mazo MA, Shamaev MY, Balabaev NK, et al. Conformational mobility of carbosilane dendrimer: Molecular dynamics simulation. Physical Chemistry and Chemical Physics. 2004;**6**:1285-1289

[30] Okrugin B, Neelov I, Borisov O, Leermakers F. Structure of asymmetrical peptide dendrimers: Insights given by self-consistent field theory. Polymer. 2017;**125**:292-302

[31] Shavykin OV, Neelov IM, Darinskii AA. Is the manifestation of the local dynamics in the spin–lattice NMR relaxation in dendrimers sensitive to excluded volume interactions? Physical Chemistry Chemical Physics. 2016;**18**:24307-24317

[32] Falkovich S, Markelov D, Neelov I, Darinskii A. Are structural properties of dendrimers sensitive to the symmetry of branching? Computer simulation of lysine dendrimers. Journal of Chemical Physics. 2013;**139**:064903

[33] Neelov IM, Markelov DA, Falkovich SG, Ilyash MY, Okrugin BM, Darinskii AA. Mathematical modeling of lysine dendrimers. Temperature dependencies. Vysokomolec. Soed. Ser. A, 2013;**55**:963-970

[34] Shypshyna MS, Veselovsky NS, Myasoedov NF, Shram SI, Fedulova SA. Effect of peptide Semax on synaptic activity and short-term plasticity of glutamatergic synapses of co-cultured dorsal root ganglion and dorsal horn neurons. Fiziologicheskiĭ Zhurnal. 2015;**61**:48-55

[35] Shevchenko KV, Nagaev IY, Alfeeva LY, Andreeva LA, Kamenskii AA, Levitskaya NG, Shevchenko VP, Grivennikova IA, Myasoedov NF. Kinetics of semax penetration into the brain and blood of rats after its intranasal administration. Russian Journal of Bioorganic Chemistry. 2006;**32**(1):57-62

[36] Ashmarin IP, Samonina GE, Lyapina LA, Kamenskii AA, Levitskaya NG, Grivennikov IA, Dolotov OV, Andreeva LA, Myasoedov NF. Natural and hybrid ("chimeric") stable regulatory glyproline peptides. Pathophysiology. 2005;**11**:179-185

[37] Kozina LS, Arutjunyan AV, Stvolinskii SL, Havinson VH. Evaluation of the biological activity of regulatory peptides in model in-vitro experiments. Successes of Gerontology. 2008;**21**:68-73

[38] Havinson VH, Bondarev IE, Butjugov AA. Epithalon enduces telomerase activity and telomeres elongation in human somatic cells. Bulletin of Experimental Biology and Medicine. 2003;**135**(6):692-695

[39] Petkova AT, Yau WM, Tycko R. Experimental constraints on quaternary structure in Alzheimer's β-amyloid fibrils. Biochemistry. 2006;**45**:498-512

[40] Paravastu AK, Leapman RD, Yau WM, Tycko R. Molecular structural basis for polymorphism in Alzheimer's β-amyloid fibrils. Proceedings of the National Academy of Sciences of the United States of America. 2008;**105**:18349-18354

[41] Klajnert B, Cladera J, Bryszewska M. Molecular interaction of dendrimers with amyloid peptides: pH dependences. Biomacromolecules. 2006;**7**:2186-2191

[42] Sadovnichy V, Tikhonravov A, Voevodin V, Opanasenko V, editors. Contemporary high performance computing: From petascale toward exascale. Boca Raton, United States: Wiley and Sons; 2013. p. 283-307

IntechOpen